Journal of Materials Chemistry A

Accepted Manuscript

ROYAL SOCIETY OF CHEMISTRY

www.rsc.org/materialsA

Journal Name

ARTICLE

One-dimensional periodic mesoporous organosilica helical nanotube with amphiphilic property for removal of contaminants in water

Received 00th January 20xx,
Accepted 00th January 20xx

DOI: 10.1039/x0xx00000x

www.rsc.org/

Houbing Zou,[a] Runwei Wang,*[a] Zhiqiang Shi,[a] Jinyu Dai, [a] Zongtao Zhang,*[a] and Shilun Qiu[a]

In this work, we report one new class of one-dimensional highly uniform periodic mesoporous organosilica (PMO) helical nanotubes with unique amphiphilic framework and perpendicular mesochannels in wall through a simple, efficient and controllable one-step strategy. The chiral mesoporous silica (CMS) nanorods were used as hard templates. The evolution of nanotube sturcture involved a process of organosilane-directed growth-induced etching, in which the growth of external PMO wall promoted the dissolution of internal CMS nanorod, and the dissolved silicate species transformed into the external PMO wall by co-condensation with hydrolyzed organosilane oligomers. Moreover, the helical mophlogy was retained completely in the process of sturctutral evolution. In addition, PMO helical nanotube with different aspect ratio, wall thickness and curvature as well as chemical composition could be easily prepared via this strategy. Furthermore, the PMO helical nanotube exhibited well amphiphilicity and can be served as a particle emulsifier for fabricating Pickering emulsions with different morphologies in various systems. Most importantly, the PMO helical nanotube showed outstanding performance in removal of hydrophobic contaminants from water, whose sorption capacity (1800～3000 mg/g) was much higher than mesosilica nanotube and conventional MCM-41, and even comparable to some sponges.

1. Introduction

Hollow porous nanostructures have received increasing concerns[1–7] and have been widely applied in many important research fields such as nanoreactors,[8–18] drug/gene delivery,[19–23] surface-enhanced Raman scattering technologies,[24] and energy storage in lithium-ion batteries[25–29] because of their unique properties resulting from permeable shells and interstitial hollow spaces with controlled functionalities. Generally, several synthetic strategies for designing and fabricating such a hollow porous nanostructure have been developed, including the Kirkendall or Ostwald ripening effects,[30-31] ship-in-bottle techniques,[32] bottom-up approaches using soft templating assemblies,[33-36] selective etching methods using hard templates[37-38] and self-templating.[39-40] However, because of the great availability of spherical templates which are energetically favored to form, the most common hollow nanostructures are hollow spheres so far, which are pseudo-zero-dimensional (0D) materials. On the other hand, one-dimensional (1D) tubular nanostructures are especially interesting because they not only have a high geometrical aspect ratio producing anisotropic features for special applications, but also can be served as novel basic building blocks for nanodevices and possible hard templates for 1D nanostructures with different chemical compositions.[41-45] Therefore, 1D hollow nanostructures are also particularly appealing to researchers for their potential properties and applications.

Silica nanotubes present one special class of one-dimensional (1D) hollow nanostructure and have attracted great attention since its first report in 1995.[46] Currently, there are several strategies available for preparing such silica nanotubes, which can be broadly categorized into anisotropic hard template methods and soft template methods. Inorganic nanorods/nanowires including gold,[47] silver,[48] nickel,[49] ZnO,[50] and Bi_2S_3,[51] were successively used as hard templates to prepare silica nanotubes. Channels in porous anodic aluminum oxide were also viewed as smart reactors for synthesis of silica nanotubes through confined growth.[52-53] Recently, crystalline nanorods of a nickel-hydrazine complex formed in reverse micelles were even used as anisotropic hard templates for gram-scale synthesis silica nanotubes with high uniformity and controllable aspect ratio.[44-45] However, these methods all involved in a multiple process of coating silica - selective etching of templates. Moreover, there are not any nanopores in the wall of these silica nanotubes, which results in the less availability of the interstitial hollow interior. On the other hand, various amphiphilic surfactants such as sodium dodecyl sulfate (SDS),[54-55] N-Dodecyl-N,N-dimethyl-3-ammonio-1-propanesulfonate (DDAPS),[56] and even self-designed chiral low-molecular-weight amphiphiles[57-61] have been developed as soft templates to prepared silica nanotubes with mesoporous walls. Among them, there is a unique type of mesostructure, which possesses a helical ordered mesopore arrangement around the tubes.[54,56] Unfortunately, the mesochannels in wall of these silica nanotubes almost were parallel to the central axis of tube, which

[a] State Key Laboratory of Inorganic Synthesis and Preparative Chemistry, College of Chemistry, Jilin University, 2699 Qianjin Street, Changchun, 130012, China. E-mail: rwwang@jlu.edu.cn, zzhang@jlu.edu.cn.

Electronic Supplementary Information (ESI) available: [details of any supplementary information available should be included here]. See DOI: 10.1039/x0xx00000x

largely limited the application in loading guest molecules.

More challengingly, the inert silica framework of these nanotubes is fully hydrophilic and shows less functionality. Periodic mesoporous organosilicas (PMOs), on the other hand, are reported as a new class of molecularly organic–inorganic hybrid nanoporous silica material with a comparably ordered pore structure and much higher hydrothermal stability.[62-64] Various bridged organic groups in pore wall can not only provide unique hydrophilicity/hydrophobicity, but also support designing desired functionality for special applications. Over the past several years, we have witnessed that the 0D hollow structured PMO nanosphere was developed as a special class of multifunctional hollow mesoporous silica nanomaterials[65] and showed more potential in the field of sorption, catalysis[16-18] and bio-medicine[66-67]. Undoubtedly, introducing some polar/functional organic groups into the framework and creating more accessible mesochannels in the wall will endow silica nanotube more opportunities in practical applications and even in new research horizon. Therefore, constructing highly uniform hybrid silica nanotubes with unique hydrophilicity/hydrophobicity and perpendicular mesochannel in wall via a simple, efficient and controllable one-step route is highly desirable for improving and further exploring their practical applications.

Herein, we report one new class of highly uniform periodic mesoporous organosilica (PMO) helical nanotubes with unique amphiphilic framework and perpendicular mesochannels in wall. The chiral mesoporous silica (CMS) nanorods were used as hard templates but our synthesis only involved an outstanding process of growth-induced etching,[68] which is a simple, efficient and highly controllable one-step strategy. To the best of our knowledge, this is the first time that hybrid silica nanotubes with unique hydrophilicity/hydrophobicity and perpendicular mesochannel in wall have been reported. The structural parameters such as aspect ratio, wall thickness and curvature, and the chemical composition were highly controllable via adjusting the synthesis conditions. Moreover, this PMO helical nanotube showed well amphiphilicity and could be served as a particle emulsifier for forming Pickering emulsions with different morphologies. Importantly, owing to the unique amphiphilic framework and perpendicular mesochannels in wall as well as the interistial 1D hollow cavity, they exhibited outstanding performance in removal of hydrophobic contaminants from water.

2. Experimental Section

2.1. Chemicals

Tetraethylorthosilicate (TEOS, 98%) and aqueous ammonia ($NH_3{\cdot}H_2O$, 25-28%) were purchased from Sinopharm Chemical Reagent Co.Ltd. 1,2-bis(triethoxysilyl)ethane (BTEE, 97%) and triblock copolymer Pluronic F127 ($EO_{100}PO_{70}EO_{100}$, EO＝ethylene oxide, PO＝propylene oxide) were obtained from Sigma–Aldrich. Bis(triethoxysilyl)methane (BTEM, 96%) was purchased from J&K Scientific. Cetyltrimethyl-ammonium bromide (CTAB, 99.0 %) was obtained from Huishi Biochemical Reagent Company of China. All chemicals were used as received without any further purification.

2.2. Synthesis of -Et- Bridged Periodic Mesoporous Organosilica (Et-PMO) Helical Nanotube

In a typical synthesis, 0.123 g of F127 and 0.3 g of CTAB were dissolved in a mixture containing 29 mL of water and 1 mL of $NH_3{\cdot}H_2O$ (25-28 %) to form a colorless and transparent solution, to which 0.3 mL of TEOS was added under stirring. After stirring at room temperature for 2 hours, a white suspension formed, and 0.3 mL of organosilane BTEE was solwly dropwise added. And then, the as-obtained white mixture was transferred to a stainless steel autoclave with a Teflon container and hydrothermally treated at 100 ℃ for 24 hours after completely hydrolysis of BTEE. The Et-PMO helical nanotube was collected by high-speed centrifugation and then washed with water and ethanol for several times. The surfactant CTAB and F127 were removed by refluxing 0.5 g of as-made material in 100 mL of ethanol containing 1.5 g of concentrated HCl aqueous solution for 6 hours.

0.183 g of CTAB led to Et-PMO helical nanotube with littler aspect ratio, 0.4 mL of organosilane BTEE led to Et-PMO helical nanotube with thicker tube wall, and 1.5 mL of aqueous ammonia led to Et-PMO helical nanotube with enhanced curvature.

The Me-PMO helical nanotube was prepared under the identical conditions for Et-PMO helical nanotube except replacing the organosilane BTEE with organosilane BTEM. The mesosilica nanotube nanotube was prepared via calcining the Et-PMO helical nanotube at 550 ℃ for 6 h.

2.3. Absorption of Hydrophobic Contaminants in Water

50 μL of organic solvent including benzene, toluene, nitrobenzene, styrene and chlorobenzene was added to 6 mL of water containing 15 mg of different absorbents (Et-PMO helical nanotube, mesosilica nanotube and MCM-41). The absorption was carried out in a sealed glass vial by equilibrating the mixture for 3 h on a magnetic stirring apparatus. The amount of organic solvent in water was measured with a UV/Vis spectroscopy.

2.4. Characterization

SEM was performed on a JEOL JSM-6700F field-emission electron microscope. TEM images were obtained on an FEI Tecnai G2 F20s-twin D573 field-emission transmission electron microscope with an accelerating voltage of 200 kV. Powder XRD patterns were obtained by using a Rigaku 2550 diffractometer with Cu Ka radiation (λ=1.5418 A). N_2 adsorption–desorption isotherms were obtained at -196 ℃ on a Micromeritics ASAP 2010 sorptometer. Samples were degassed at 120 ℃ for a minimum of 12 h prior to analysis. Brunauer–Emmett–Teller (BET) surface areas were calculated from the linear part of the BET plot. The pore size distribution was estimated from the adsorption branch of the isotherm by the BJH method. The total pore volume was estimated from the adsorbed amount at P/P_0 = 0.995. The IR spectra were acquired using a Bruker IFS 66 V/S FTIR spectrometer. ^{29}Si CP-MAS NMR measurements were performed on a Bruker AVANCE III 400 WB spectrometer. The spinning rate was 12 kHz and a total number of 20000 scans were recorded with a 6 s recycle delay for each sample. ^{13}C-MAS NMR measurements were performed on a Varian Infinity Plus 400 NMR spectrometer. The spinning rate was 4 kHz and a total number of 800 scans were recorded with a 4 s recycle delay for each sample. UV-vis spectra were recorded with a Shimadzu UV-2450 spectrometer.

3. Results and discussion

3.1. Preparation and Characterization of Et-PMO Helical Nanotube

The -Et- bridged periodic mesoporous organosilica (Et-PMO) helical nanotube was prepared using the chiral mesoporous silica (CMS) helical nanorod as the hard template (Fig.1a). Firstly, the CMS helical nanorod with the length of 700～800 nm and the diameter of 80～100 nm (Fig.S1A) was fabricated using achiral surfactants CTAB and F127 as the templates according to the previous publications.[69-70] After a hydrothermal process followed simply introduction an organisilane BTEE into the pristine solution

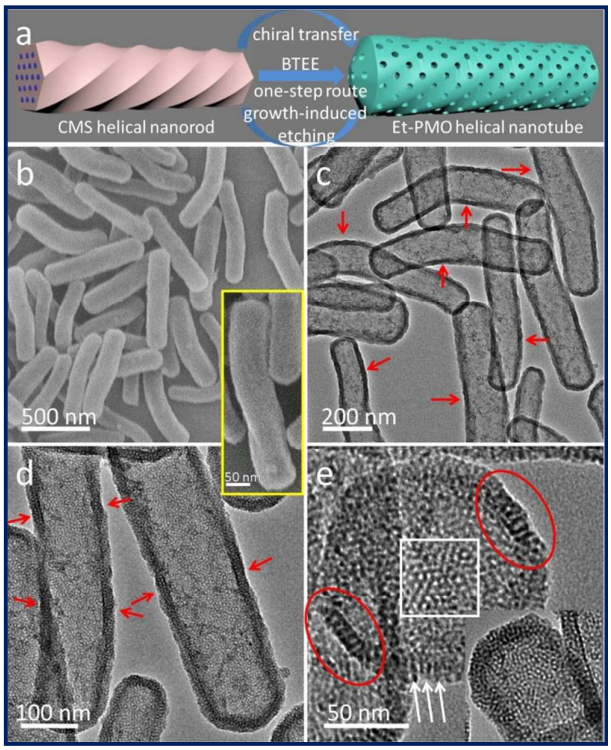

Figure 1. (a) Schematic illustration for the formation of Et-PMO helical nanotube from CMS helical rod. (b) Low-magnification SEM image and (c) TEM image of Et-PMO helical nanotube; the inset in (b) high-magnification SEM image of single left-handed Et-PMO helical nanotube; (d), (e) and the inset in (e) high-magnification TEM images of Et-PMO helical nanotube taken with the incident beam perpendicular or parallel to the nanotube, respectively.

of as-formed CMS, well defined Et-PMO helical nanotube was formed. From the SEM images in Fig.1b and Fig.S1B, we can clearly observe that the obtained materials are highly uniform nanorod. The length and the diameter are approximately 700～800 nm and 120 nm, respectively. The TEM image (Fig.1c) further confirms that the materials have a nanotube structure with a uniform wall thickness of 16 nm. Moreover, the high-magnification SEM image (the inset in Fig.1b) reveals that the nanotube is obviously twisted, and this individual nanotube is left-handed according to previous reports. [63-64] The helicity of this nanotube was further characterized by TEM. In the HRTEM image taken with the incident beam perpendicular to the nanotube (Fig.1c, d), some dark contrasts (directed by red arrows), which are the indicative of chiral nanomaterials according to previous reports,[54-55,70-72] are clearly seen in every nanotube. The helical pitch along the nanotube axis is estimated to be 190～270 nm from the distance between two sets of dark region. Meanwhile, the image taken with the incident beam parallel to the nanotube (Fig.1e) distinctly exhibits a hexagonal hollow structure and two dark regions in the symmetrical position of hexagon (directed by red ellipses) resulting from the twisted wall, which further confirms the helical nanotube structure. Furthermore, we find that the dark contrast moves downward or upward with sample titling (Fig.S2), demonstrating the spiral nature of the tubal wall and cavity. Additionally, from the area of wall in Fig.1e and the inset, it is clear that the mesochannels in Et-PMO wall are partly ordered and perpendicular to the central axis of nantube. And a hexagonal pattern, similar to the [110] direction of MCM-41,[73] can be clearly seen in the centre area of the hollow interior, corresponding to the white boxed area in Fig.1e. We should be aware that only the Et-PMO wall and the cavity are twisted, some chirality on nanoscale level, and the mesochannels in Et-PMO wall are achiral. Note also that the whole tube is closed-ended, which will be in favor of loading guest molecules and nanoparticles, and even confined synthesis of nanostructured materials. These results demonstrate that we have successfully prepared a highly uniform Et-PMO helical nanotube with radially oriented mesochannel in wall using CMS nanorod as the hard template via a simple one-step growth-induced etching process.

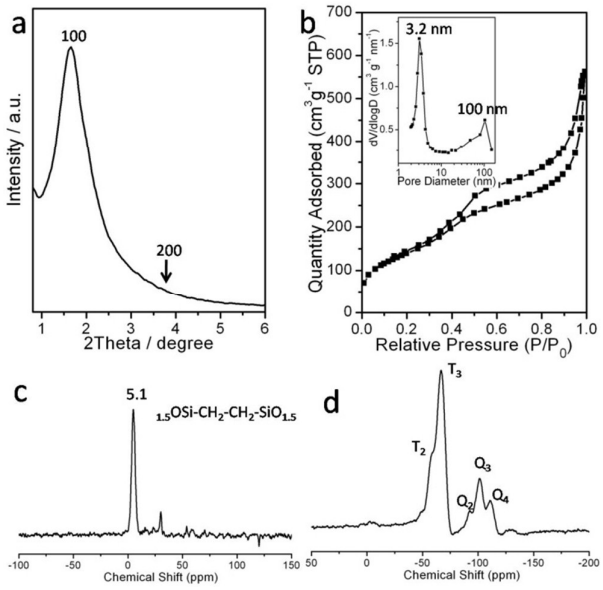

Figure 2. Small-angle XRD pattern (a), N_2 sorption isotherm (b), relevant BJH pore size distribution (the inset in b), ^{13}C NMR (c) and ^{29}Si NMR (d) spectra of Et-PMO helical nanotube.

The meso-macroporous bimodal porous structure of the Et-PMO helical nanotube is further confirmed by small-angle X-ray diffraction and nitrogen sorption analysis (Fig.2a, b). The small-angle XRD pattern exhibits one sharp diffraction peak and one weak diffraction peak at 2θ values of approximately 1.8 and 3.6 degrees (Fig.2a), indicating an partly ordered mesopore array in the Et-PMO wall. The nitrogen sorption isotherm (Fig.2b) shows a type IV curve with two sharp capillary condensation steps in the P/P_0 range of 0.3

~1.0. The capillary condensation step at the P/P_0 of ~0.4 is an indication of typical uniform mesopores in the wall, whereas the capillary condensation step occurring in the P/P_0 range of 0.6~1.0 is probably attributed to the existence of macroporous tubal cavity. Additionally, the distinct H3 hysteresis loop in the P/P_0 range of 0.4 ~1.0 indicates that the pores in the Et-PMO wall directly open into the hollow interior, supporting the idea that a guest molecule can quickly diffuse into the hollow space without any obstacle. Furthermore, the corresponding Barrett–Joyner–Halenda (BJH) pore size distribution curve (the inset in Fig.2b) shows two uniform pore sizes centered at 3.2 nm and 100 nm, respectively, which directly proves the meso-macroporous bimodal nanoporous structure. The Brunauer–Emmett–Teller (BET) surface area and the total pore volume are 512 $m^2 g^{-1}$ and 0.66 $cm^3 g^{-1}$, respectively.

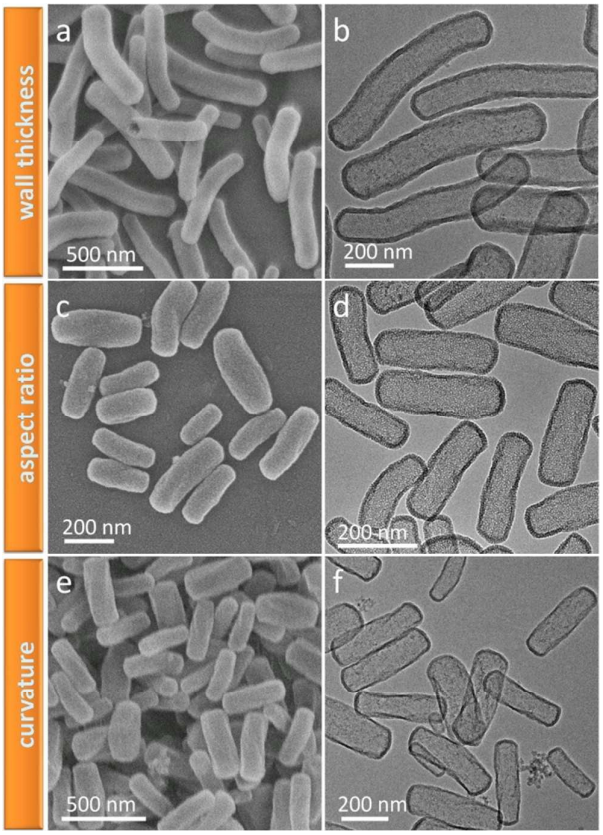

Figure 3. SEM and TEM images of Et-PMO helical nanotube with different structure parameter: (a, b) Et-PMO helical nanotube with thicker wall of 25 nm; (c, d) Et-PMO helical nanotube with littler aspect ratio of 3-4; (e, f) Et-PMO helical nanotube with larger curvature.

The chemical composition of Et-PMO helical nanotube is characterized using FT-IR, solid-state ^{13}C NMR, and ^{29}Si NMR spectroscopy (Fig.2c, d, S3). Three bands in the range of 2892–2980 cm^{-1}, at 1410 cm^{-1}, and at 1160 cm^{-1} appear in the FT-IR spectrum (Fig.S3), which we assign to the C–H stretching vibration, C–H vibration and Si–C vibration, respectively. This result indicates that ethylene groups have been incorporated into the sample. The appearance of resonance at 5.1 ppm in the ^{13}C NMR spectrum (Fig.2c), which can be attributed to the C species of the ethylene moiety, further proves the incorporation and integrity of the ethylene organic groups in the PMO wall. Moreover, the ^{29}Si NMR spectrum shows the existence of both T^n and Q^n sites in the range of -50 to -70 ppm and -90 to -115 ppm (Fig.2d), which we attribute to $SiC(OSi)_2(OH)$ (T^2 δ -62) and $SiC(OSi)_3$ (T^3 δ -67) species of silicon attached to ethylene, and the $(HO)_2Si(OSi)_2$ (Q^2 δ -93), $(HO)Si(OSi)_3$ (Q^3 δ -102) and $Si(OSi)_4$ (Q^4 δ -111) silicon species, respectively. The appearance of Q^n sites demonstrates that the dissolved silica species from CMS helical nanorod probably co-condensed with hydrolyzed organosilane oligomers and then were transformed into the external Et-PMO wall, which is similar with our previous results.[43] Additionally, the high proportion of T^n (1 : 0.3) reveals the much high hydrothermal stability of Et-PMO helical nanotube.

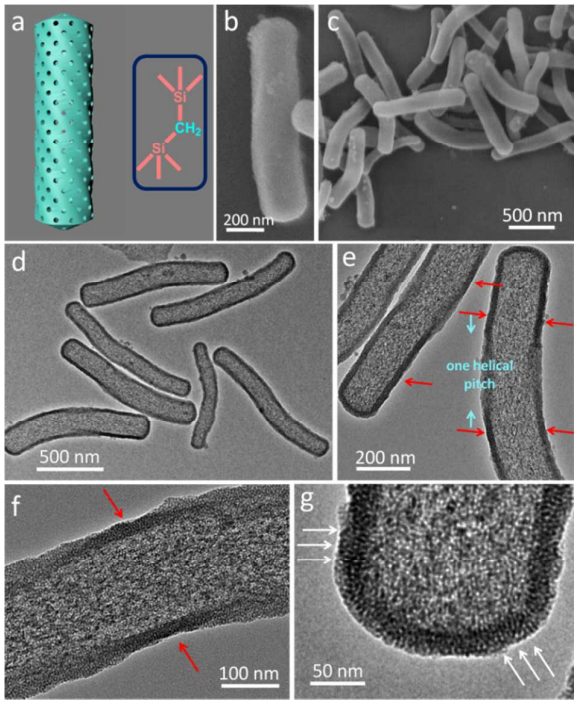

Figure 4. (a) Built model of Me-PMO helical nanotube. (b) High-magnification SEM image of single right-handed Me-PMO helical nanotube. Low-magnification SEM (c), TEM (d, e) and HRTEM (f, g) images of Me-PMO helical nanotube.

3.2. Controllable Synthesis of PMO Helical Nanotube with Different Structural Parameters and Chemical composition

We further demonstrate that the uniform Et-PMO helical nanotube with different structure parameters could be easily prepared through this strategy (Fig.3), owing to the simple and highly controllable synthesis of CMS.[69-70] Firstly, the wall thickness can be easily tailored by adjusting the amount of organosilane BTEE. For example, the thickness of wall increases to 25 nm as the amount of BTEE increases from 0.3 mL to 0.4 mL (Fig.3a, b). Moreover, decreasing the amount of surfactant CTAB in initial mixture results in CMS helical nanorod with littler aspect ratio, [69-70] and thus the Et- PMO helical nanotube with littler aspect ratio of 3-4 (Fig.3c, d, e, f). Importantly, the curvature of helical nanotube can be also tuned by adjusting the alkalinity of initial mixture. When the amount of aqueous ammonia is increases to 1.5 mL, the curvature

of obtained Et-PMO helical nanotube is distinctly enhanced (Fig.3e, f). This tailor in structure parameters will endow this one-dimensional hollow nanostructured materials more opportunities for application in relevant fields.

We also tried to prepare PMO helical nanotube with other chemical compositions. When replacing the BTEE with another organosilane BTEM under the same conditions for Et-PMO helical nanotube, the -Me- bridged PMO (Me-PMO) helical nanotube could be also formed. The low-magnification SEM image (Fig.4c) shows the highly uniform nanorod morphology. The length and the diameter are approximately 80 ～ 1000 nm and 200 nm, respectively. And the high-magnification SEM image (Fig.4b) distinctly proves the nanorod is twisted. Moreover, the TEM images (Fig.4d, e, f, g) further confirm that the materials have a twisted nanotube structure with a uniform wall thickness of 23 nm. The typical dark contrasts (directed by red arrows) are clear visible in every nanotube, and the helical pitch estimated from the distance between two sets of dark region is 200～300 nm (Fig.4e). In addition, the oriented mesochannels (directed by white arrows) can be clearly observed in the wall and end of Me-PMO helical nanotube (Fig.4g). The nitrogen sorption analysis further confirmed the uniform mesopore structure (2.9 nm) in the Me-PMO wall (Fig.S4). The chemical composition of the Me-PMO helical nanotube was confirmed by solid-state ^{13}C NMR, and ^{29}Si NMR spectroscopy (Fig.S5). These results reveal that PMO helical nanotube with various chemical compositions can be easily prepared. In addition, fully hydrophilic mesosilica nanotubes with perpendicular mesochannels in wall can be obtained via calcining these hybird PMO helical nanutubes at 550 ℃ for 6 h (Fig.S6). All above results clearly reveal that the current strategy is simple, efficient and highly controllable.

3.3. Formation Mechanism of Et-PMO Helical Nanotube

In order to investigate the formation mechanism, we used XRD, nitrogen sorption analysis, SEM and TEM to monitor the synthesis process of Et-PMO helical nanotube. Firstly, after introduction and completely hydrolysis of organosilane BTEE, well-defined core-shell structured CMS@Et-PMO helical nanorod with a wall of 16 nm was formed, as shown in the SEM and TEM images (Fig.5a, b). The small-angel XRD pattern also reveals the formation of mesostructure in Et-PMO wall (Fig.S7). From the relevant HRTEM image (Fig.5b, c), we can clearly observe that the position of the Et-PMO wall's dark regions directed by the red arrows keep full consistent with that of the CMS nanorod's (10) fringes in every CMS@Et-PMO helical nanorod. These results indicate that the external Et-PMO wall has obtained helicity from CMS helical nanorod at this stage, considering into the fact that as-obtained Et-PMO nanoparticles under the same condition for CMS don't exhibit any chirality in the morphology and mesostructure (Fig.S9). After crystallizing at 373 K for 1 h, the internal CMS nanorod is gradually dissolved, leading to a large unordered mesoporous structure, while the Et-PMO wall further grows to 23 nm (Fig.5d, e). And the CMS nanorod is almost completely dissolved out after further reacting for 4 h (Fig.5g, h). In addition, we should be aware that the helicity of external Et-PMO wall is maintained during the evolution of nanotube structure (Fig.5c, f, i). In the small-angel XRD patterns (Fig.S7), we can also clearly observe the formation of Et-PMO wall's partly ordered mesostructure and the gradual decomposition and disappearance of CMS's highly ordered mesostructure. Moreover, in the nitrogen

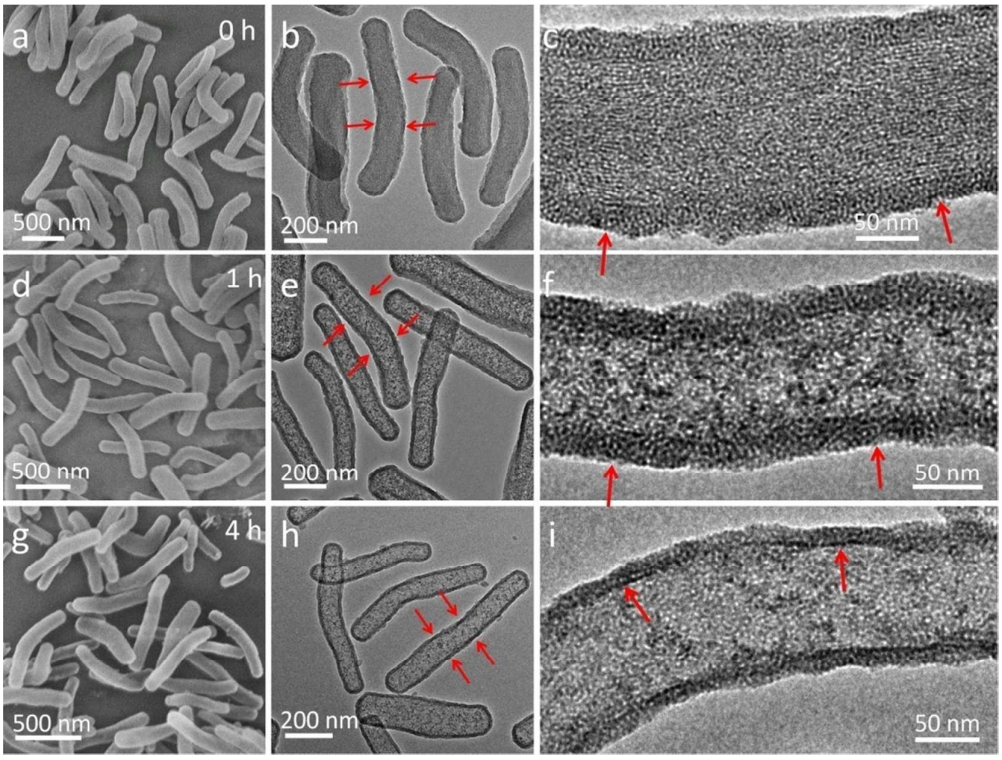

Figure 5. SEM, low-magnification TEM and high-magnification TEM images of the samples under various reaction times at 100℃: (a, b, c) 0 h; (d, e, f) 1 h; (g, h, i) 4 h.

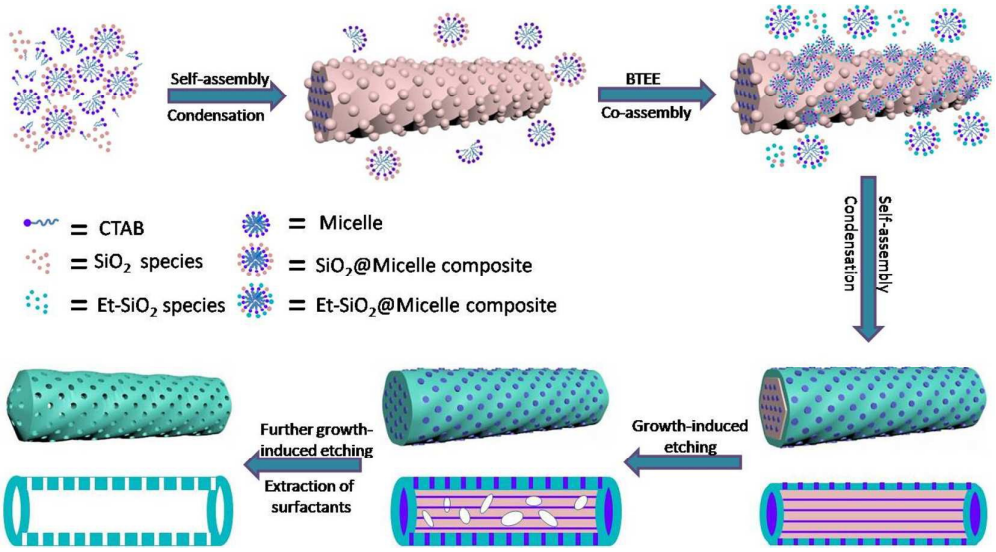

Scheme 1. Schematic illustration for the formation mechanism of the Et-PMO helical nanotube.

sorption isothermals (Fig.S8a), the hysteresis loop gradually transforms to H3 type and moves to high relative pressure P/P_0 range. The formation of mesopore structure of 3.2 nm in Et-PMO wall, the disappearance of mesopore structure of 2.8 nm in CMS nanorod, and the formation and disappearance of unordered mesopore structure of 18 nm can be further identified in the BJH pore size distribution curves (Fig.S8b), respectively. These results reveal that the CMS nanorod is first dissolved to form a large unordered mesopore structure of 18 nm, and finally is dissolved out completely.

Based on above results, we can conclude that the structural evolution of helical nanotube involves a process of organosilane-directed growth-induced etching similar with our previous reported strategy.[68] The possible formation process is illustrated in Scheme 1. Firstly, the CMS helical nanorod is prepared using achiral surfactant CTAB as template in ammonia solution, whose formation mechanism could be explained by the entropically driven model.[70] Because the CMS nanorod is as-formed in the pristine solution, the Si-OH on the every face is highly active and can further react with silica species including hydrolyzed TEOS oligomers and hydrolyzed BTEE oligomers. After the addition and hydrolysis of organisilane BTEE, BTEE-oligomers@CTAB-micelle composites fast form via co-assembly, and can further co-condense with the Si-OH arranging in a helical way on every face of CMS nanorod. And thus the composites deposit on the every face of CMS nanorod in a helical way, respectively. After further self-assembly and condensation, the helicity of the external Et-PMO wall is obtained. In other words, the Si-OH on the faces of CMS helical nanorod induce the self-assembly and the helical arrangement of BTEE-oligomers@CTAB-micelle composites through covalent bond-linked interaction. After a thin layer of Et-PMO is successfully coated on the CMS nanorod and the synthesis system is transformed to high crystallizing temperature (373 K), the internal SiO_2 nanorod starts to be selectively uniformly dissolved out due to the higher hydrothermal stability of PMO materials.[68] At the same time, the dissolved silica species transform into Et-PMO wall by co-condensation with hydrolyzed BTEE oligomers, as indicated by the result of ^{29}Si NMR spectrum (Fig.4). The internal SiO_2 nanorod is continuously dissolved, and the external Et-PMO wall further grows simultaneously. Finally, the SiO_2 nanorod is completely dissolved out, leading to the formation of nanotube structure. During the evolution process of nanotube sturctutre, the helicity of the external Et-PMO wall is always retained integrally.

3.4. Amphiphilic property of Et-PMO Helical Nanotube

We have reported that the prepared hollow nanospheres through this growth-induced etching strategy exhibited amphiphilic due to the co-existence of hydrophobic bridged organic group and hydrophilic SiO_2 unit.[18, 68] Here, the hydrophobicity/hydrophilicity of Et-PMO helical nanotube is further examined. The Et-PMO helical nanotube can disperse well in water (Fig.6a), and well W/O emulsion, as expected, can form when using cyclohexane to extract the material in water (Fig.6b). Likewise, well W/O emulsion can be also obtained when using water to extract the material in cyclohexane, although the material cannot disperse well in cyclohexane (Fig.6c, d). It is worth mentioning that no material can be observed in water after extractions. Moreover, we used other hydrophobic solvents such as octane (Fig.6e), toluene (Fig.6f) and nitrobenzene (Fig.6g) to extract material in water, and similar phenomenon of emulsification can be also observed. Furthermore, the relevant optical microscopy images of W/O emulsions in cyclohexane-water (Fig.6C), octane-water (Fig.6D) and toluene-water (Fig.6E) distinctly show uniformly spherical morphology, which is comparable with that of W/O emulsion in cyclohexane-water using surfactant CTAB as emulsifier (Fig.6G). More interestingly, W/O emulsion with rod morphology, as shown in the Fig.6F, can be obtained in the nitrobenzene-water system using our prepared Et-PMO helical nanotube as particle emulsifier. To the best of our knowledge, this is the first time for the fabrication of emulsion with rod morphology using nanoparticle as emulsifier. These different emulsions can remain stable for no less than one month (Fig.S10), suggesting that these emulsions can be applied as templates for fabricating various nanostructures such as hollow spheres and tubes with different chemical composition.

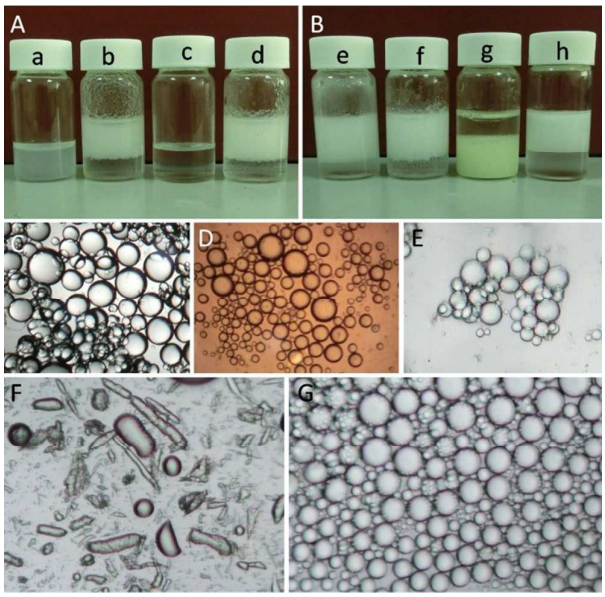

Figure 6. Digital photographs of (A), (a) Et-PMO helical nanotube dispersed in water, (b) cyclohexane extracting Et-PMO helical nanotube dispersed in water, (c) Et-PMO helical nanotube dispersed in cyclohexane, (d) water extracting Et-PMO helical nanotube in cyclohexane; (B), W/O emulsions in various systems of (e) octane-water, (f) toluene-water, (g) nitrobenzene-water and (h) octane-water; the Et-PMO helical nanotube was used as particle emulsifier in (e, f, g) and the surfactant CTAB was used as emulsifier in (h). (C), (D), (E), (F), (G) Microphotographs of various W/O emulsions in above (b), (e), (f), (g) and (h), respectively.

Meanwhile, we also examined the emulsification between liquid (water) and gas (air) using the Et-PMO helical nanotube as emulsifier. From the photograph in the Fig.S11c, it can be clearly seen that some foam that can be seen as air/water emulsion form on the liquid surface after drastic shock, similar with the phenomenon using surfactant CTAB as emulsifier (Fig.S11d). However, similar phenomenon cannot be observed using MCM-41 nanoparticle (Fig.S11b). In addition, after standing for 4 days without disturbance, this foam still exists, but most of foam has disappeared in the case of CTAB (Fig.S11e, f), which suggests that this amphiphilic helical nanotube can be even served as a stable foaming agent. Based on all these results, this Et-PMO helical nanotube shows superior amphiphilicity, which can be applied as an excellent particle emulsifier for preparing emulsions with various morphologies, and will be potential in the field of Pickering interfacial catalysis.[74-75]

3.5. Application of Et-PMO Helical Nanotube in Removal of Contaminants in Water

Amphiphilic nanomaterials are viewed as excellent collectors for hydrophobic contaminant in water because they can disperse well in water and have strong affinity to hydrophobic organics.[18,68,76] This Et-PMO nanotubes exhibit unique structural features including the amphiphilic framework, the perpendicular mesochannels in wall and the macroporous 1D hollow cavity. Hence, we investigated the applications of the Et-PMO helical nanotubes in removal of hydrophobic contaminants in water. Various toxic organic solvents

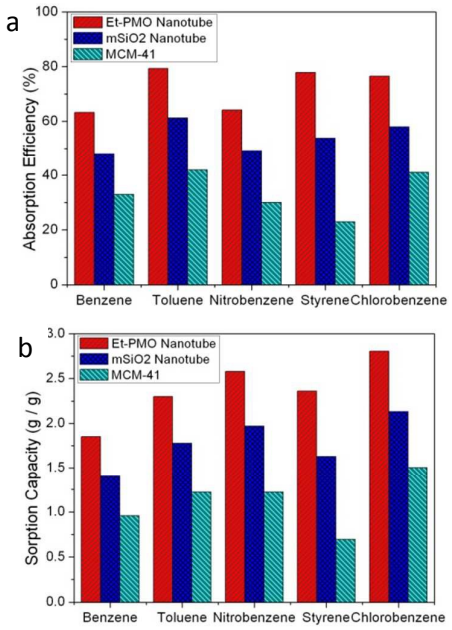

Figure 7. The sorption efficiency (a) and sorption capacity (b) of Et-PMO nanotube, mesosilica nanotube and conventional MCM-41 for various hydrophobic contaminants in water, including benzene, toluene, nitrobenzene, styrene and chlorobenzene.

including toluene, nitrobenzene, and chlorobenzene, which are well known as toxic organic contaminants in water treatment, were tested, and the results are shown in the Fig.7 and Fig.S12. The Et-PMO nanotubes absorbed 70%～80% of organics from aqueous after a short sorption time (3 h), whereas the sorption efficiencies of mesosilica nanotubes only reached to 40%～60% (Fig.7a). Obviously, considering their similarity in structure (Fig.S6), the much higher absorption performance of Et-PMO nanotubes should be attributed to their unique amphiphilic properties. We and others have also reported that amphiphilic framework has strong affinity to hydrophobic organics.[18,68,76] Moreover, the sorption efficiencies of Et-PMO and mesosilica nanotube are distinctly higher than that of conventional MCM-41, which should be attributed to the accessible mesochannel in wall and macroporous hollow cavity. These results cleary indicate that the mesochannels in wall are highly accessible and the interstitial 1D hollow cavity is available. Most interestingly, the sorption capacity of Et-PMO nanotubes has reached to 1800～3000 mg/g (Fig.7b), which is 2～3 times of conventinal MCM-41 material and even comparable to some sponges[77-78] that are generally viewed as one class of advanced materials for removal of organic pollutants from water and oil/water seperation. It is also worthy mentioning that the sorption capacity of Et-PMO nanotube is much higher than the total pore volume of the material (0.66 cm^3 g^{-1}), indicating that most of contaminants are stored in the macroporous cavity of nanotube, which further proving the highly accessible mesochannels in wall and the interstitial hollow cavity support the applications in loading guest molecules and even nanoparticles. All these data clearly demonstrate that this Et-PMO nanotube is a superior absorbent for removal of contaminants in water. Because of the unique amphiphilic framework, perpendicular mesochannels in wall and

the interstitial 1D hollow cavity, we believe that this reported PMO helical nanotube will have great potentials in waste water treatment and templated-synthesis, bio-medicine and catalysis particular in interfacial catalysis.

4. Conclusions

In summary, we have reported one new class of one dimensional highly uniform PMO helical nanotubes with unique amphiphilic framework and perpendicular mesochannels in wall prepared using CMS helical nanorods as the hard templates via a simple and efficient one-step strategy of growth-induced etching. The structural parameters including aspect ratio, wall thickness and curvature and chemical composition are highly controllable. Moreover, these PMO helical nanotubes exhibited well amphiphilic property and could be used as particle emulsifiers for preparing Pickering emulsions with different morphologies of sphere or rod in various systems. Most importantly, owing to the unique amphiphilic framework and perpendicular mesochannels in wall as well as the interistial 1D hollow cavity, this PMO helical nanotube can be used as a surperior absorbent and showed outstanding performance in removal of various hydrophobic contaminants from water. Because of the simple and controllable fabrication process and their outstanding structural properties, we believe that these amphiphilic 1D hollow porous nanostructured materials will have great potentials in various applications such as water treatments, templated-synthesis, bio-medicine and Pickering interfacial catalysis.

Acknowledgements

This work was supported by National Natural Science Foundation of China (21390394), the National Basic Research Program of China (2012CB821700, 2011CB808703), NSFC (21261130584, 91022030), “111” project (B07016), Award Project of KAUST (CRG-1-2012-LAI-009) and Ministry of Education, Science and Technology Development Center Project (20120061130012).

Notes and references

1 J. Liu, N. P. Wickramaratne, S. Z. Qiao and M. Jaroniec, *Nat. Mater.,* 2015, **14,** 763-744.
2 J. Liu, S. Z. Qiao, J. S. Chen, X. W. Lou, X. R. Xing and G. Q. Lu, *Chem. Commun.,* 2011, **47,** 12578-12591.
3 Y. Li and J. Shi, Adv. Mater., 2014, **26,** 3176-3205.
4 Y. Chen, H. Chen and J. Shi, *Acc. Chem. Res.,* 2013, **47,** 125-137.
5 X. Li, Y. Yang and Q. H. Yang *J. Mater. Chem. A,* 2013, **1,** 1525-1535.
6 X. L. Fang, X. J. Zhao, W. J. Fang, C. Chen and N. F. Zheng, *Nanoscale,* 2013, **5,** 2205-2218.
7 Z. Wang, L. Zhou and X. Lou, *Adv. Mater.,* 2012, **24,** 1903-1911.
8 K. Kamata, Y. Lu and Y. N. Xia, *J. Am. Chem. Soc.,* 2003, **125,** 2384-2385.
9 P. M. Arnal, M. Comotti and F. Sch¨uth, *Angew. Chem., Int. Ed.,* 2006, **45,** 8224-8227.
10 J. Lee, J. C. Park and H. Song, *Adv. Mater.,* 2008, **20,** 1523-1528.
11 L. F. Tan, D. Chen, H. Y. Liu and F. Q. Tang, *Adv. Mater.,* 2010, **22,** 4885-4889.
12 S. Wu, J. Dzubiella, J. Kaiser, M. Drechsler, X. Guo, M. Ballauff and Y. Lu, *Angew. Chem., Int. Ed.,* 2012, **51,** 2229-2233.
13 J. Gaitzsch, D. Appelhans, L. Wang, G. Battaglia and B. Voit, *Angew. Chem., Int. Ed.,* 2012, **51,** 4448-4451.
14 X. L. Fang, Z. H. Liu, M. F. Hsieh, M. Chen, P. X. Liu, C. Chen and N. F. Zheng, *ACS Nano,* 2012, **6,** 4434-4444.
15 B. Y. Guan, X. Wang, Y. Xiao, Y. L. Liu and Q. S. Huo, *Nanoscale,* 2013, **5,** 2469-2475.
16 J. Liu, H. Q. Yang, F. Kleitz, Z. G. Chen, T. Y. Yang, E. Strounina, G. Q. Lu and S. Z. Qiao, *Adv. Funct. Mater.,* 2012, **22,** 591-599.
17 Y. Yang, X. Liu, X. Li, J. Zhao, S. Bai, J. Liu and Q. H. Yang, *Angew. Chem.,* 2012, **124,** 9298-9302.
18 H. B. Zou, R. W. Wang, J. Y. Dai, Y. Wang, X. Wang, Z. T. Zhang and S. L. Qiu, *Chem. Commun.,* 2015, **51,** 14601-14604.
19 K. An and T. Hyeon, *Nano Today,* 2009, **4,** 359-373.
20 Y. Chen, H. R. Chen, L. M. Guo, Q. J. He, F. Chen, J. Zhou, J. W. Feng and J. L. Shi, *ACS Nano,* 2010, **4,** 529-539.
21 Y. Chen, P. F. Xu, H. R. Chen, Y. S. Li, W. B. Bu, Z. Shu, Y. P. Li, J. M. Zhang, L. X. Zhang, L. M. Pan, X. Z. Cui, Z. L. Hua, J. Wang, L. L. Zhang and J. L. Shi, *Adv. Mater.,* 2013, **25,** 3100-3105.
22 Y. Chen, Q. Meng, M. Wu, S. Wang, P. Xu, H. Chen, Y. Li, L. Zhang, L. Wang and J. Shi, *J. Am. Chem. Soc.,* 2014, **136,** 16326−16334
23 X. Li, L. Zhou, Y. Wei, A. M. El-Toni, F. Zhang and D. Zhao, *J. Am. Chem. Soc.,* 2015, **137,** 5903−5906.
24 M. Roca and A. J. Haes, *J. Am. Chem. Soc.,* 2008, **130,** 14273-14279.
25 L. Zhang, H. B. Wu, B. Liu and X. W. Lou, *Energy Environ. Sci.*, 2014, **7**, 1013-1017.
26 L. Zhang, H. B. Wu, Y. Yan, X. Wang and X. W. Lou, *Energy Environ. Sci.*, 2014, **7**, 3302-3306.
27 G. Zhang, H. B. Wu, T. Song, U. Paik and X. W. Lou, *Angew. Chem. Int. Ed.,* 2014, **53,** 12590–12593.
28 H. Ren, R. Yu, J. Wang, Q. Jin, M. Yang, D. Mao, D.d Kisailus, H. Zhao and D. Wang, *Nano Lett.,* 2014, **14,** 6679–6684.
29 Z. Dong, H. Ren, C. M. Hessel, J. Wang, R. Yu, Q. Jin, M. Yang, Z. Hu, Y. Chen, Z. Tang, H. Zhao and D. Wang, *Adv. Mater.,* 2014, **26,** 905–909.
30 Y. Yin, R. Rioux, C. Erdonmez, S. Hughes, G. Somorjai and A. Alivisatos, *Science,* 2004, **304**, 711-714.
31 J. Li and H. Zeng, *J. Am. Chem. Soc.,* 2007, **129**, 15839-15847.
32 M. Xiao, C. Zhao, H. Chen, B. Yang and J. Wang, *Adv. Funct. Mater.,* 2012, **22**, 4526-4532.
33 H. Djojoputro, X. F. Zhou, S. Z. Qiao, L. Z. Wang, C. Z. Yu and G. Q. Lu, *J. Am. Chem. Soc.,* 2006, **128,** 6320-6321.
34 J. Liu, S. Qiao, S. Hartono and G. Lu, *Angew. Chem. Int. Ed.,* 2010, **49**, 4981-4985.
35 X. Wu and D. Xu, *J. Am. Chem. Soc.,* 2009, **131**, 2774-2775.
36 X. Wu and D. Xu, *Adv. Mater.,* 2010, **22**, 1516-1520.
37 G. Qi, Y. Wang, L. Estevez, A. Switzer, X. Duan, X. Yang and E. Giannelis, *Chem. Mater.,* 2010, **22**, 2693-2695.
38 Y. Yang, J. Liu, X. Li, X. Liu and Q. Yang, *Chem. Mater.* 2011, **23**, 3676-3684.
39 X. Fang, X. Zhao, W. Fang, C. Chen and N. Zheng, *Nanoscale*, 2013, **5**, 2205-2218.

40 Z. Teng, X. Su, Y. Zheng, J. Sun, G. Chen, C. Tian, J. Wang, H. Li, Y. Zhao and G. Lu, *Chem. Mater.* 2013, **25**, 98-105.
41 R. Fan, Y. Wu, D. Li, M. Yue, A. Majumdar and P. Yang, *J. Am. Chem. Soc.*, 2003, **125,** 5254–5255.
42 Y. N. Xia, P. D. Yang, Y. G. Sun, Y. Y. Wu, B. Mayers, B. Gates, Y. D. Yin, F. Kim and H. Q. Yan, *Adv. Mater.,* 2003, **15,** 353–389.
43 P. Sajanlal, T. Sreeprasad, A. Samal and T. Pradeep, *Nano Reviews,* 2011, **2,** 5883.
44 C. Gao, Z. Lu and Y. Yin, *Langmuir,* 2011, **27,** 12201–12208
45 C. Gao, Q. Zhang, Z. Lu and Y. Yin, *J. Am. Chem. Soc.,* 2011, **133,** 19706–19709
46 H. Nakamura and Y. Matsui, *J. Am. Chem. Soc.*, 1995, **117,** 2651-2652.
47 S. Obare, N. Jana and C. Murphy, *Nano Lett.,* 2001, **1,** 601-603.
48 Y. Yin, Y. Lu, Y. Sun and Y. Xia, *Nano Lett.,* 2002, **2,** 427–430.
49 K. S. Mayya, D. I. Gittins, A. M. Dibaj and F. Caruso, *Nano Lett.,* 2001, **1,** 727–730.
50 Y. Chen, X. Xue and T. Wang, *Nanotechnology,* 2005, **16,** 1978–1982.
51 S. F. Wang, F. Gu, Z. S. Yang, M. K. Lu, G. J. Zhou and W. G. Zou, *J. Cryst. Growth,* 2005, **282,** 79–84.
52 X. Yang, H. Tang, K. Cao, H. Song, W. Sheng and Q. Wu, *J. Mater. Chem.,* 2011, **21,** 6122–6135.
53 W. Lee and S.-J. Park, *Chem. Rev.*, 2014, **114,** 7487–7556.
54 X. Wu, J. Ruan, T. Ohsuna, O. Terasaki, S. Che, *Chem. Mater.,* 2007, **19,** 1577-1583.
55 X. Wu and C. Crudden, *Chem. Mater.,* 2012, **24,** 3839−3846.
56 X. Wu, Y. Jiang and D. Xu, *J. Phys. Chem. C,* 2011, **115,** 11342-11347.
57 Y. Chen, B. Li, X. Wu, X. Zhu, M. Suzuki, K. Hanabusa and Y. Yang, *Chem. Commun*., 2008, 4948-4950.
58 X. Liu, W. Zhuang, B. Li, L. Wu, S. Wang, Y. Li and Y. Yang, *Chem. Commun.,* 2011, **47,** 7215-7217.
59 B. Li, Z. Xu, W. Zhuang, Y. Chen, S. Wang, Y. Li, M. Wang and Y. Yang, *Chem. Commun.,* 2011, **47,** 11495-11497.
60 C. Zhang, Y. Li, B. Li and Y. Yang, *Chem. Asian J.,* 2013, **8,** 2714-2720.
61 Y. Li, B. Li, Z. Yan, Z. Xiao, Z. Huang, K. Hu, S. Wang and Y. Yang, *Chem. Mater.,* 2013, **25,** 307-312.
62 T. Asefa, M. J. MacLachlan, N. Coombs and G. A. Ozin, *Nature* 1999, **402**, 867-871.
63 N. Mizoshita, T. Tani and S. Inagaki, *Chem. Soc. Rev.* 2011, **40,** 789-800.
64 P. Van Der Voort, D. Esquivel, E. De Canck, F. Goethals, I. Van Driessche and F. J. Romero-Salguero, *Chem. Soc. Rev.* 2013,**42**, 3913-3955.
65 J. G. Croissant, X. Cattoën, M. W. C. Man, J. Durand, and N. M. Khashab, *Nanoscale,* 2015, **7,** 20318–20334.
66 Y. Chen, Q. Meng, M. Wu, S. Wang, P. Xu, H. Chen, Y. Li, L. Zhang, L. Wang, and J. Shi, *J. Am. Chem. Soc.,* 2014, **136,** 16326−16334.
67 Z. Teng, X. Su, Y. Zheng, J. Zhang, Y. Liu, S. Wang, J. Wu, G. Chen, J. Wang, D. Zhao, and G. Lu, *J. Am. Chem. Soc.,* 2015, **137,** 7935–7944.
68 H. Zou, R. Wang, X. Li, X. Wang, S. Zeng, S. Ding, L. Li, Z. Zhang and S. Qiu, *J. Mater. Chem. A,* 2014, **2,** 12403-12412.
69 J. Ye, H. Zhang, R. Yang, X. Li and L. Qi, *Small* 2010, **6,** 296-306.
70 Y. Han, L. Zhao and J. Ying, *Adv. Mater.,* 2007, **19,** 2454-2459.
71 Y. Zhu, J. He, C. Shang, X. Miao, J. Huang, Z. Liu, H. Chen and Y. Han, *J. Am. Chem. Soc.,* 2014, **136,** 12746-12752.
72 H. Qiu and S. Che, *Chem. Soc. Rev.,* 2011, **40,** 1259-1268.
73 B. Tan and S. Rankin, *J. Phys. Chem. B,* 2004, **108,** 20122-20129.
74 H. Yang, L. Fu, L. Wei, J. Liang and B. Binks, *J. Am. Chem. Soc.,* 2015, **137,** 1362-1371.
75 M. Pera-Titus, L. Leclercq, J.-M. Clacens, F. De Campo and V. Nardello-Rataj, *Angew. Chem., Int. Ed.,* 2015, **54,** 2006-2021.
76 Y. Guan, X. Meng and D. Qiu, *Langmuir,* 2014, **30,** 3681-3686.
77 A. Li, H. Sun, D. Tan, W. Fan, S. Wen, X. Qing, G. Li, S. Li and W. Deng, *Energy Environ. Sci.,* 2011, **4,** 2062-2065.
78 L. Li, B. Li, L. Wu, X. Zhao and J. Zhang, *Chem. Commun.,* 2014, **50,** 7831-7833.

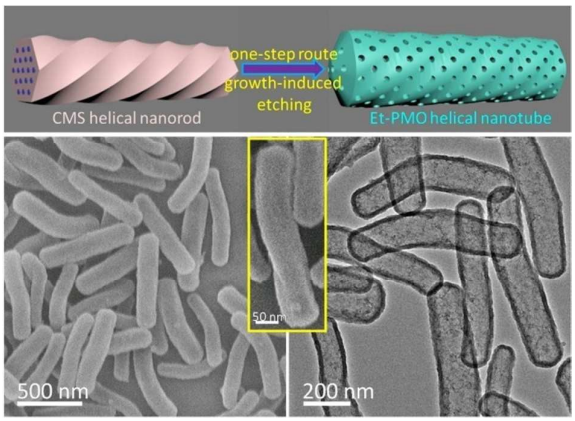

One new class of one dimensional highly uniform periodic mesoporous organosilica helical nanotube with unique amphiphilic framework and perpendicular mesochannels in wall has been reported via a simple, efficient and controllable one-step strategy of growth-induced etching. This nanotube shows outstanding performance in removal of hydrophobic contaminants from water.